Numerical simulation of Two-dimensional risers under oscillatory flows with low Reynolds and KC for predicting the involve forces response

***M. Catalina Valencia-Cárdenas and C. A. Riveros**

School of Engineering, Research group GEOc, Universidad de Antioquia, Colombia.
* Presenting author: mcatalina.valencia@udea.edu.co

ABSTRACT

This research implements a numerical simulation of flexible risers under oscillatory flows initially at rest. A single freedom degree spring-mass-damper system is employed with low mass allowed to move only in cross-flow direction. Two-dimensional incompressible Navier-Stokes equations are discretized using the Finite Volume Method (FVM). To resolve the pressure-velocity linkage, an iterative solution strategy SIMPLEC algorithm for transient problems is used. To study the influence of smaller Reynolds values on the dynamic system, a critic value KC=7,9 is fixed. For Reynolds less than 300, the system behavior is in agreement with the literature, where a direct relationship between the force and the vortex shedding is presented. An almost null cross-flow force appear for Re=40 which becomes important as increased the Reynolds value, changing between fluctuating and stabilizing force. From Reynolds 300 the cross-flow force is very chaotic and some discrepancies with literature appear in the system dynamics. The numerical results obtained from the proposed numerical base approach show good agreement with experimental data collected from a flexible riser model according to the spectral analysis.

Keywords: *Flexible riser, Keulegan-Carpenter number, oscillating flow, numerical simulation, vortex dynamics*

1. Introduction

The structural movement by external variable velocity flow is a very common phenomenon in flexible risers but there is still a limitation to accurately predicting the response of these structures. This is due to most of the prediction models rely heavily on large experimental databases. In addition, flexible and light materials have been developing for marine applications leading to slender structures with low mass ratios. This characteristic facilitates the structure movement caused by vortex shedding for incoming flow. In many real cases, the flow can be oscillating in a sinusoidal mode and Reynolds (Re) and Keulegan-Carpenter (KC) dimensionless numbers can describe this behavior. Here $Re = U_m D/\nu$ and $KC = U_m T/D$, where ν is the kinematic viscosity, U_m is the amplitude of the oscillatory flow velocity, T is the oscillatory flow period and D is the diameter of the cylinder. Their importance regards in the relationship between these numbers and the forces that causing the structure movement. The cross-flow force exerted onto the structure is particularly harmful, exerting a significant dynamic stress, increasing the damage accumulation and eventually causing structural failure.

The frequency at which the vortices are shear is known as vortex shedding frequencies (f_v); a regular pattern of vortices induces fluctuating lift and drag forces on the cylinder [1]. The shedding frequency and both forces become constant for Reynolds number intervals, which means the heavy influences of this number on the cylinder maximum response ([2] [3]). Many authors have been researching its influence until a value of 500, considering a fixed value for KC ([4], [5], [6], [7], [8], [9], [10], [11]). Tatsuno and Bearman [12] analyzed $1.6 < KC < 15$ and $5 < \beta < 160$ ($\beta = Re/KC = D^2/\nu T$), including three-dimensional features, provided the identification of eight regimes denoted from A to G in a plane (KC, R_e). This classification has become the standard description for the associated flow regimes. The regimen A corresponds to the Williamson`s symmetrical regimen [13], that is also similar to Regime B but with an axial direction three-dimensional structure. Regime C corresponds to vortices of opposite rotation senses in the same fashion of a Von Kármán vortex street. Regime D exhibits a symmetrical V-pattern around the transverse axis, very similar to regime E, however here the V-pattern changes intermittently its direction from one side to the other. Regime F describes the Williamson`s double pair regime [13], whereas the Williamson`s transverse street is similar to Regime G. Finally, the Tatsuno and Bearman [12] regimen classification suggests that a KC such as 7,9 that crosses five different regimens, can be assumed as critical and important to be studied.

This study describes and discusses the resulting forces by oscillating fluid flow effect around a cylinder under the influence of a fixed KC (7,9) and Re between 40 and 1000, considering lower mass ratio and covering the most Tatsuno and Bearman regimes (A, D, E, F and G). The cylinder-oscillating period is implemented for a long time (more than fifty cycles) in order to analyze the flow patterns in each regime. A single degree of freedom system with a spring-mass-damper is implemented, where the mass is allowed to move only in cross-flow direction. To discretize the transport equations, the Finite Volume Method (FVM) is used and to resolve the pressure-velocity linkage, an iterative solution strategy SIMPLEC algorithm for transient problems is used. Moreover, a bi-dimensional model is established using OpenFOAM simulations and employing a single desktop computer. The results presented here consider an experimental validation [14] in order to demonstrate the use of numerical based approaches to predict the response of flexible risers.

In what follows, Section 2 presents the numerical method description with the respective equations modeling, parameters taking account, computational domain, boundary conditions and model validation. Section 3 put forward a discussion of the force characterization according to the transitions between regimes established for different intervals of Reynolds values. In addition, the results are compared with experimental data in this section. A study summary is presented in Section 4.

2. Numerical method

To model the vortex generation around a structure, commonly a sinusoidal oscillatory flow is considered to represent a realistic phenomenon representation. The flow in the longitudinal direction is given by:

$$U_1(t) = U_m sin(2\pi t/T) \qquad (1)$$

The oscillating flow considered is controlled by 40, 100, 150, 200, 250, 300, 500 and 1000 as Reynolds numbers and 7,9 as Keulegan Carpenter number, so eight different regimens were simulated. Other parameters (mass, damping, reduced velocity) are set up to allow the cylinder movement according to Valencia-Cardenas, M. [15].

A discretized form of two-dimensional incompressible Navier-Stokes equations must be defined at a nodal point placed within each control volume in order to solve the problem. OpenFOAM, an open source solver, is used to solve the governing equations selecting adequate solution schemes in order to achieve reliable results. To reach it, a second-order central difference scheme is used for the convection and diffusion terms. A stable and accurate simulation is obtained by choosing an implicit second-order scheme for temporal discretization. For the numerical procedure in the simulation, to improve the pressure and velocity coupling, the PIMPLE algorithm is utilized [16].

The structure is allowed to move only perpendicularly to the flow direction. To apply the transport equations to the inertial system, time to time and according to the cylinder movement, the numerical grid is moved and adjusted. For that reason, a mesh dynamic motion solver is implemented in the model, where the cylinder is constrained to only move along “y” and cannot rotate. Finally, the total force per unit length by a stationary cylinder under a oscillatory flow F_{osc} is known as Morison’s equation [17], written as:

$$F_{osc}(t) = \rho C_m \frac{\pi}{4} D^2 \dot{U}(t) + \frac{1}{2}\rho C_D D |U(t)| U(t) \tag{2}$$

Where ρ represents the fluid density, C_m the inertia coefficient and C_D the drag coefficient. The last two are functions of R_e and KC.

The computational domain is a cylinder in a channel represented using two-dimensional numerical simulations as shown in Figure 1. The cylinder is represented as a circle with diameter D submersed in an incompressible fluid, represented here as a rectangular flow domain. As the simulation begins, the center body is located at the center of the coordinate’s axis, 10D from the horizontal walls and 20D from the vertical walls. The domain areas around the cylinder, where the vortices are shed, contains a higher cell density in order to obtain a better resolution. This region is shaped by four arcs whose radius equal $2.5\sqrt{2}D$.

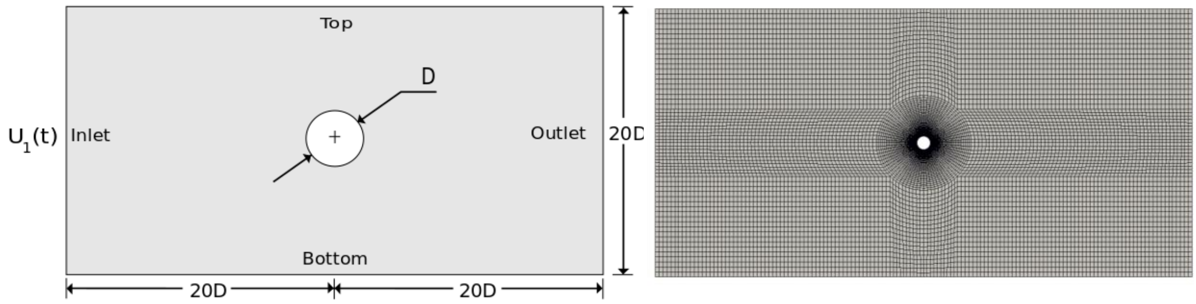

Figure 1. Sketch and computational mesh of oscillating flow around circular cylinder

To guarantee the smallest numerical errors, it is necessary to proof the meshing independently. The test is developed from a course mesh established, using a non-dimensional time step $U_1\Delta_t/D = 0{,}1$ (where Δ_t is time step) as sufficient condition to ensure coefficients with three significant digits [18]. Then, the mesh is refined consecutively and the time step is determined from the Courant number (c_o) expression, $c_o = |U_1|\Delta_t/\Delta_x$ where Δ_x is the smaller cell size in the velocity direction and c_o is defined as 0.2 [19]. Finally, the appropriate mesh is selected taking into account the fitting between results and literature and the tradeoff between precision and computational cost (see Figure 1).

Table 1. Comparison of drag force coefficient (x̄=1.307, 95% CI [1.281, 1.332]) and Strouhal number (x̄=0.193, 95% CI [0.187, 0.198]) at $Re = 200$ and $KC = 10$

	$\bar{C}_D$	S_t
Guilmineau and Queutey (2002)	1.286	0.195
Cao et al. (2010)	1.300	0.186
Cao and Li (2015)	1.343	0.191
Present work	1.331	0.192

In order to guarantee an accurate solution, the model is setting up at values of Reynolds and Keulegan Carpenter well studied in the literature (e.g. [18], [20], [10], [21]). The drag and lift coefficients time history and the Strouhal number are analyzed, considering 20 vortex shedding periods once the periodic flow is stablished. These values have been compared with published results ([10], [21], [22]) and shown in Table 1.

The drag coefficient (mean value of the in-line non-dimensionalized force) and the Strouhal number, $S_t = f_v D/U_m$, are obtained from the frequency of vortex shedding f_v, which is calculated with the period measured from velocity time history. At $Re = 200$ and $KC = 10$, $\bar{C}_D$ is equal to 1.331 and S_t is equal to 0.192, meaning that the vortex natural frequency shedding is f_0 =0.192. Results are in good agreement with those published in the literature (see Table 1).

3. Results and discussions

The results of direct numerical simulation are presented in this section considering the effect of $KC = 7{,}9$ and Reynolds values equals to 40, 100, 150, 200, 250, 300, 500 and 1000. In this work, the regimes are defined from the flow structure and force behavior.

3.1.In-line and transverse forces

Drag and lift coefficients time histories in an oscillating flow are estimated using force coefficients function library by OpenFOAM. Vortex shedding frequencies and Strouhal numbers obtained for different Reynolds values are shown in Figure 2. The time history frequencies are verified for both drag and lift coefficients in order to obtain the vortex shedding frequency, using the Fast Fourier Transform method (FFT) [20]. The dominant frequency corresponds to the oscillating frequency.

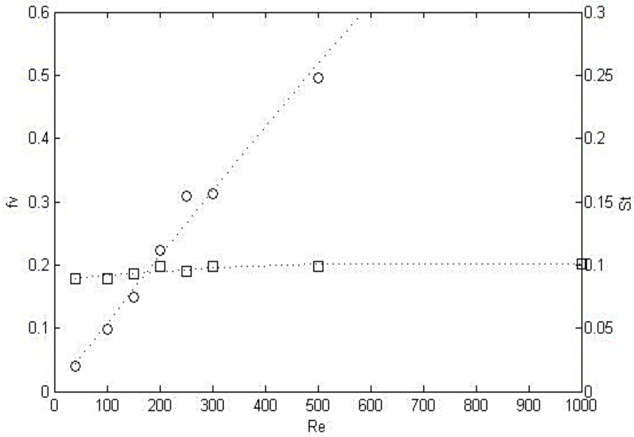

Figure 2. Vortex shedding frequencies (circle) and Strouhal numbers (square) by Reynolds number

The semi-empirical Eq. (2) estimate the in-line force on a cylinder divided in two forces: 1) The drag force, proportional to the flow instantaneous velocity square and 2) the inertial flow coupled with the local flow acceleration [22]. The drag force coefficient C_d and the inertial force coefficient C_m can be obtained by last square fifting on the time history of F_{osc}, or calculated using the equations below [23].

$$C_d = \frac{3}{4}\int_0^{2\pi} \frac{F_D \sin\theta}{\rho D U_1^2}\, d\theta = \frac{3}{8}\int_0^{2\pi} C_D \sin\theta\, d\theta \tag{3}$$

$$C_m = \frac{2U_1T_f}{\pi^3 D}\int_0^{2\pi}\frac{F_D\cos\theta}{\rho D U_1^2}d\theta = \frac{U_1T_f}{\pi^3 D}\int_0^{2\pi}C_D\cos\theta\, d\theta \quad (4)$$

Where, C_D represents the mean drag coefficient.

According to Cao and Li [22], the time history of drag force can be acceptably approximated by Morrison's equation. Using the same equations is possible to obtain the cross-flow force. Figure 3 shows an interval of in-line and cross-flow forces for every Reynolds value studied.

The drag and the inertial forces share a direct relation with the vortex behavior as shown in Figure 3. A uniform in-line force with almost constant frequency and period can visualized in Figure 3(a). This regimen A does not exhibits vortex detachment, but it does show a vortex formation totally symetric in the direction of the flow. This is why in-line force predominates and the trasnverse force is almost null.

A representative regimen D is showed in Figure 3(b), where the V-pattern symmetrical starts to dominate and the cross-flow force becomes important. The symmetric pattern becomes predominant when the cross-flow force amplitude reduces. The fluctuation force classify this case of Reynolds value in a symmetric regime group.

The Re=150 case present and amplitude instability due the irregular vortex shedding in Figure 3(c). After a while, the fluctuations tends to become regular and the in-line force is stabilizes. Here regimen E is predominant with intermitently changes of direction, related with the fluctuating amplitude in-line force because the action of cross-flow force. When cross-flow force present a peak, vorticity pattern tends to be transversal street.

For Re= 200, an amplitude stability is presented and persist at the time (Figure 3(d)). In the same way, the Re= 250 present a regular fluctuation force (Figure 3(e)). Also, cross-flow force present uniform behavior for both Reynolds (200 and 250). Reynolds case 200 and 250 are dominated by regimen F. In-line force for Re= 200 tends to be more stable in comparison with Re= 250 which means the first one present vortex shedding more symmetrical about the cross-flow axis while the second one tends to be more transversal. In this way, the proximity to the transition range is a bit evident for Re= 250.

For case of Reynolds 300, 500 and 1000, in-line and cross-flow forces are chaotic and strong peaks appear (see Figures 3(f)(g) and (h)). A chaotic behavior is observed here because there are no persistent vortex pattern. Sometimes, the dominant harmonic for the case of Re= 1000 are three times the frequency of oscillating fluid flow, but predominates two times the oscillating frequency. On the other hand, flow regime is dominated by the viscous drag component in all the cases.

3.2.Spectral analysis

Several oscillating fluid flow frequencies peaks that are integral times the vortex oscillating frequency, are illustrated in Figure 4 and Figure 5. These figures were obtained from time history of drag force and lift force coefficients respectively, using Fast Fourier Transform (FFT). The oscillating frequencies are graphed with the magnitude of the Fourier Transform, using the main peak as indicated Williamson [13].

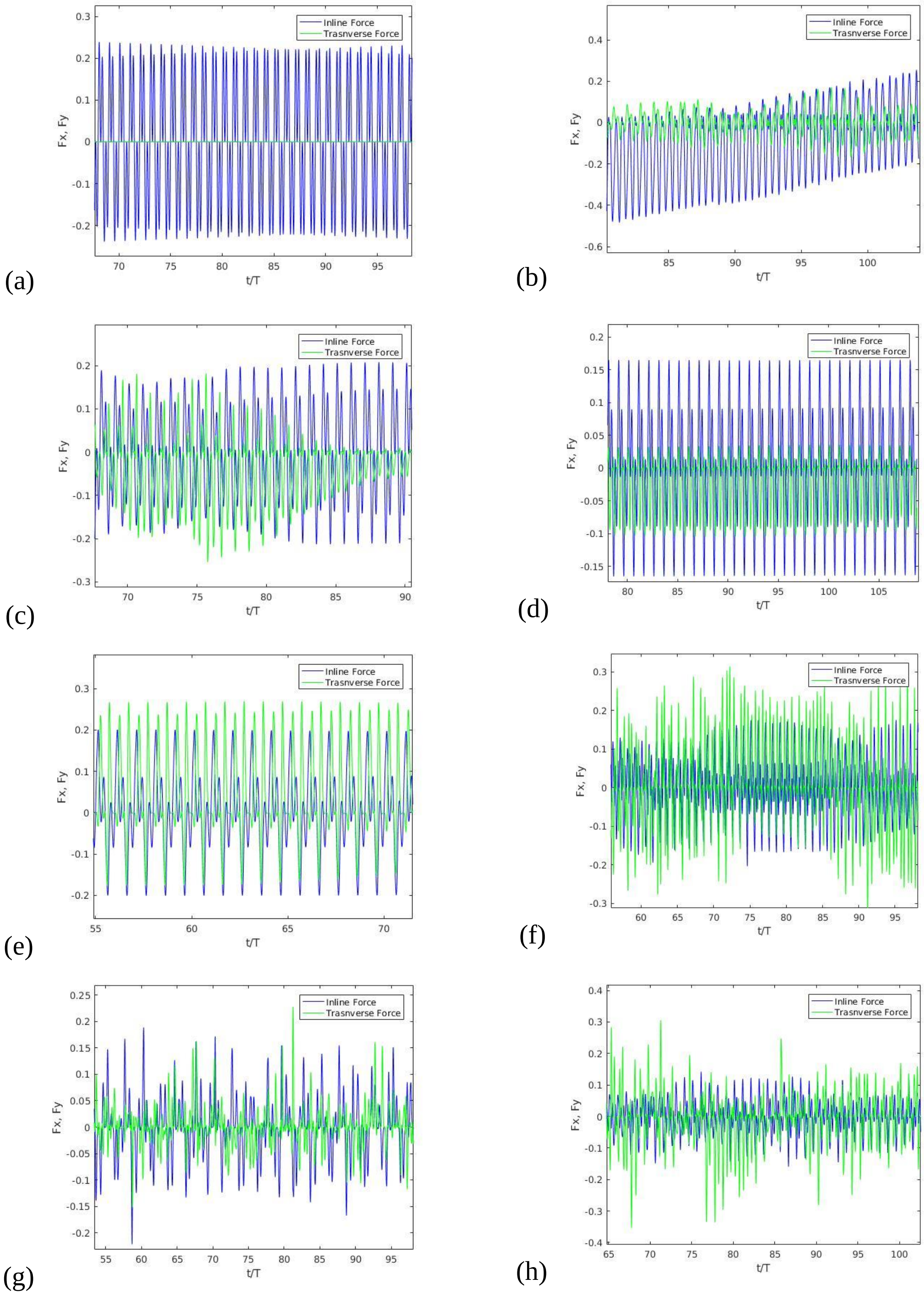

Figure 3. In-line and cross-flow forces for a) Re 40, b) Re 100, c) Re 150, d) Re 200, e) Re 250, f) Re 300, g) Re 500 and h) Re 1000.

Spetral analysis of drag force is shown in Figure 4 with several peaks at frequencies. The main frequency are always the oscillating frequency and the other peaks has an increment factor, namely $3f_0, 5f_0, 7f_0$ and in that way forward (see Figure 4(a)(b)(c)), for regimes A, D, E and

F. Besides of the main frequency and the $3f_0$ peak, other frequencies peaks without multiple of f_0 appear in regimen G.

It is possible to note, the oscillating frequencies for Reynolds values less than 200 (see Figure 4) are twice the main frequency of lift coefficient. As shown in Figures 5(a)(b), for regimes A and E respectively, the main frequencies occur with an increment of $2f_0$. Otherwise, the dominant frequency for regimen F (Figures 5(c)) is three times the oscillating frequency. In this case, the case of Reynold value 250 presents main frequency at $3f_0$ and the increment is about $1f_0$ in the others frequencies peaks.

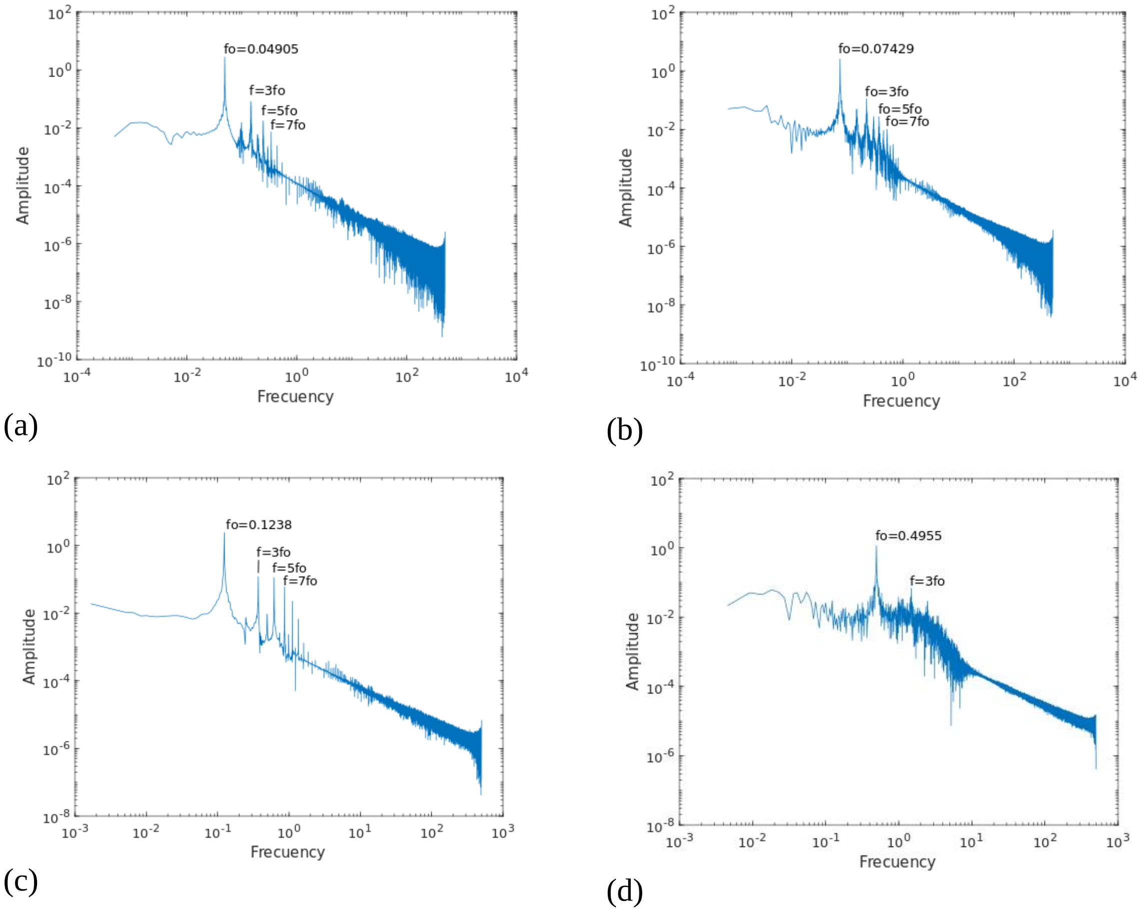

Figure 4. Spetral analysis of drag force coefficient at a) Re 100, b) Re 150, c) Re 250, d) Re 1000.

The same behavior for these regimens is shown by Duclercq et. al. [4]. Again, for Reynolds values higher than 300 the oscillating frequencies are two times the main frequency of lift coefficient. Note that the main frequency in Figures 5(d), is presented around of $2f_0$. Them appear others frequencies peaks without a clear multiple of f_0 and strong fluctuations is observed. Williamson [13] concluded that in an oscillating flow, the dominant frequency of lift force is equal to one plus the number of vortices shedding in a half period, which is evidenced in the regimes A, D and F. However, for regimen G this condition is not fulfilled as proved in this study.

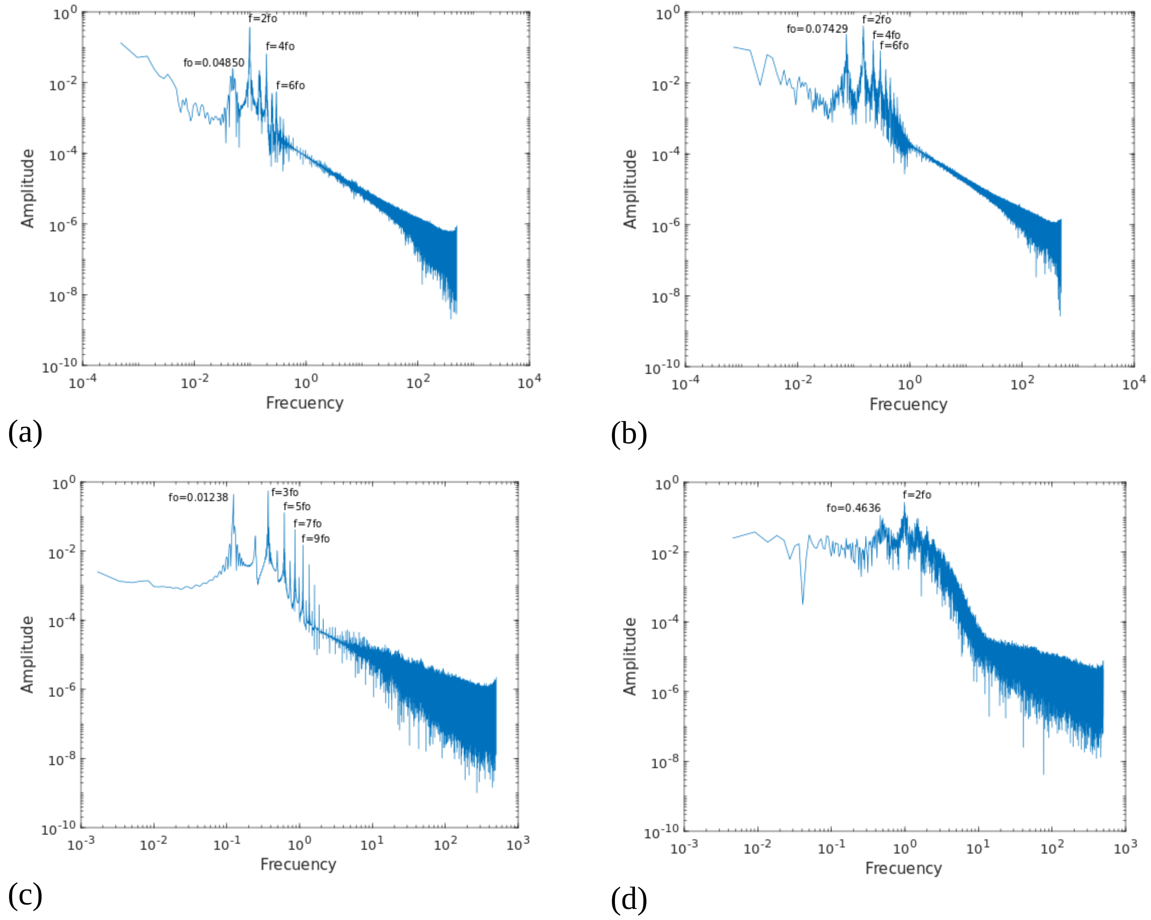

Figure 5. Spetral analysis of lift force coefficient at a) Re 100, b) Re 150, c) Re 250, d) Re 1000.

3.3.Experimental validation

Riveros et. al. [14] conducted a series of forced oscillation experiments for flexible risers where a 20-meter riser model was tested for different values of Re and KC numbers; their experimental model case 1 has the same diameter as Re (1000) and KC (7,9) numbers presented here. Although good agreement was reported by Riveros et. al. [14], it is still possible to observe some deviations between the simulation results and experimental data in the main cross-flow frequency. The model presented in this paper, as shown in Figure 4(d), overcomes this difficulty providing a value of the dominant cross-flow frequency in good agreement with the experimental value of 1 Hz presented by Riveros et. al. [14]. Likewise, the dominant inline-flow frequency presented in the experimental model by Riveros et. al. [14] is 4,9 Hz, the same visualized in Figure 4(d) using the numerical model.

4. Summary

A numerical simulation of two-dimensional risers under oscillatory flows with low Reynolds and KC for predicting the involve forces response was presented in this paper. A inverse relationship between the Reynolds number and the mean drag coefficients, is an expected behavior result [14]. Also demostrated that the peaks shape variation of forces behaviour is related with a pressure distribution asymmetry in the flow direction, due to asinchrony in the vortex shedding. Thus, the lowest Reynolds number, the less variation in amplitude and frequency parameters and conversely, the higher Reynolds numbers produces significant variations, especially in fluctuation amplitude.

Reynolds value 40 present a good agreement to the Williamson regimen with vortex symmetric formation in the flow direction which explains why the in-line force predominates and the cross-flow force is almost null. Instability develops when Reynolds value is incremented to $R_e = 100$ where transverse vortices appear. This is conforms to Tatsuno & Bearman regimen D behavior, where a symmetrical V-pattern began to develop and the cross-flow force becomes important. The V-pattern symmetrical regimen persists in the $R_e = 150$ case because changes intermittently from a transverse street to oblique street vortex. An amplitude instability is present due irregular vortex shedding, after a while, the fluctuations becomes regular and the in-line force stabilizes. Here regimen E is predominant with intermittently changes of direction, related with the fluctuating amplitude in-line force because the action of cross-flow force, this conforms to Tatsuno & Bearman.

In-line force for $R_e = 200$ tends to be more stable in comparison with $R_e = 250$, so $R_e = 200$ shows vortex shedding more symmetrical about the cross-flow axis while the second one tends to be more transversal. In this way, the proximity to the transition range is evident for $R_e = 250$. Both cases are conform to Tatsuno & Bearman regimen F behavior with regular fluctuation force and also, the cross-flow force present uniform behavior. Regimen instability appears as the Reynolds value increases (Reynolds value 300, 500 and 1000). Reynolds 300 and 500 is classified by Williamson [13] as regimen G, but transverse street is not the most persistent behavior. The pattern is considered chaotic for all these cases where there are ot persisten force patterns. In-line and cross-flow forces are chaotic and strong peaks appear. The dominant harmonic for the case of Re= 1000 sometimes is three times higher than the oscillating fluid flow frequency, but two times the oscillating frequency. The flow regime is dominated by the viscous drag component in all these cases.

Finally, the numerical results presented in this paper for the dominant in-line and cross-flow frequency shows good agreement with experimental results provided by Riveros et. al. [14].

Acknowledgements

The authors gratefully acknowledge to the reviewers, the Universidad de Antioquia and the Grupo de Estudios Oceánicos “Luis Fernando Vásquez-Bedoya” for the financing and logistic support provided to this work.

References

[1] S. Chakrabarti, "The Theory and Practice of Hydrodynamics an Vibration," *World Scientific Publishing.*, vol. 20, 2002.

[2] C. Govardhan and R. Williamson, "Defining the Modified Griffin plot in vortex-induced vibration: revealing the effect of Reynolds number using controlled damping"," *Journal of Fluid Mechanics*, vol. 561, pp. 147-180, 2006.

[3] J. Klamo, A. Leonard and A. Roshki, "On the maximum amplitude for a freely vibrating cylinder in crossflow," *Journal of Fluid and Structures*, vol. 21, pp. 429-434, 2005.

[4] M. Duclercq, D. Broc and O. Cadot, "Characterization of long time fluctuations of forces exerted on an oscillating circular cylinder at KC=10," *Journal of Fluids and Structures*, vol. 27, no. 4, pp. 18-29, 2011.

[5] J. Lin and D. Rockwell, "Quantitative interpretation of vortices," *Experiments in Fluids,* vol. 23, no. 2, pp. 99-104, 1997.

[6] P. Anagnostopoulos and G. Iliadis, "Numerical study of the flow pattern and the in-line response of a flexible cylinder in an oscillating stream," *Journal of Fluids,* vol. 12, pp. 225-258, 1998.

[7] G. Iliadis and P. Anagnostopoulos, "Viscous oscillatory flow around a circular cylinder at low Keulegan–Carpenter numbers and frequency parameters," *International Journal for Numerical Methods in Fluids,* vol. 26, p. 403–442, 1998.

[8] H. Dutsch, F. Durst, S. Becker and H. Lienhart, "Low-Reynolds-number flow around an oscillating circular cylinder at low Keulegan–Carpenter numbers," *Journal of Fluid Mechanics 360,*, vol. 260, p. 249–271, 1998.

[9] B. Uzunoglu, M. Tan and W. Price, "Low-Reynolds-number flow around an oscillating circular cylinder using a cell viscous boundary element method," *International Journal for Numerical Methods in Engineering,* vol. 50, p. 2317–2338, 2001.

[10] E. Guilmineau and P. Queutey, "A numerical simulation of vortex shedding from an oscillatory circular cylinder," *Journal of Fluids and Structures,* vol. 16, no. 6, p. 773–794, 2002.

[11] D. Nehari, V. Armenio and F. Ballio, "Three-dimensional analysis of the unidirectional oscillatory flow around a circular cylinder at low Keulegan– Carpenter and beta numbers," *Journal of Fluid Mechanics,* vol. 520, p. 157–186, 2004.

[12] M. Tatsuno and P. Bearman, "A visual study of the flow around an oscillating," *Journal,* vol. 211, pp. 157-182, 1990.

[13] C. Williamson, "Sinusoidal flow relative to circular cylinders," *Journal of Fluid Mechanics,* vol. 155, p. 141–174, 1985.

[14] C. Riveros, T. Utsunomiya, K. Maeda and K. Itoh, "Response prediction of long flexible risers subject to forced," *Journal of Marine and Science Technology,* vol. 15, pp. 44-53, 2010.

[15] M. Valencia-Cardenas, *Numerical study of uniform and oscillatory flows over a circular cylinder (M.S. thesis),* Universidad de Antioquia, 2017.

[16] C. J. Greenshields, OpenFOAM User Guide, OpenFOAM Fundation , 2017.

[17] J. Morison, M. O'Brien, J. Johnson and S. Schaaf, "The force exerted by surface waves on piles," *Journal of Candian Petroleum Technology,* vol. 189, p. 149–154., 1950.

[18] S. Étienne and D. Pelletier, "The low Reynolds number limit of vortex-induced vibrations," *Journal of Fluids and Structures,* vol. 31, pp. 18-29, 2012.

[19] J. K. Tawekal, CFD simulation of the Flow over a 2-Dimensional Pipe and Vortex Induced Vibration of the Pipe with 1 Degree of Freedom, Stavanger: University of Stavanger, 2015.

[20] Z. Pan, W. Cui and Q. Miao, "Numerical simulation of vortex-induced vibration of a circular cylinder at low mass-damping using RANS code," *Journal of Fluids and Structures,* vol. 23, pp. 23-32, 2007.

[21] S. Cao, S. Ozono, Y. Tamura, Y. Ge and H. Kikugawa, "Numerical simulation of Reynolds number effects on velocity shear flow around a circular cylinder," *Journal of Fluids and Structures,* vol. 26, p. 685–702, 2010.

[22] S. Cao and M. Li, "Numerical study of flow over a circular cylinder in oscillatory flows with zero-mean and non-zero-mean velocities," *Journal of Wind Engineering and Industrial Aerodynamics,* vol. 144, pp. 42-52, 2015.

[23] G. Keulegan and L. Carpenter, "Forces on cylinders and plates in an oscillating flui," *Journal of Research of the National Bureau of Standards 60,* vol. 60, pp. 423-440, 1958.

[24] T. Sarpkaya, "In-line and Transverse Forces on Smooth and Sand-roughened Cylinders in Oscillatory Flow at High Reynolds Numbers," *National Science Foundation,* 1976.